



Diverse ultrasound image features of unilateral genital tract obstruction with ipsilateral renal anomaly syndrome on genitourinary system segmental sequential ultrasound screening and the accuracy of ultrasonic diagnosis

Ling Zhang[^], Rong Liu[^], Ronghua Liu, Mingfu Wu, Shuangmei Ye[^]

Department of Obstetrics and Gynecology, Tongji Hospital, Tongji Medical College, Huazhong University of Science and Technology, Wuhan, China

Contributions: (I) Conception and design: L Zhang; (II) Administrative support: L Zhang, Rong Liu; (III) Provision of study materials or patients: All authors; (IV) Collection and assembly of data: L Zhang; (V) Data analysis and interpretation: All authors; (VI) Manuscript writing: All authors; (VII) Final approval of manuscript: All authors.

Correspondence to: Ling Zhang, MM. Department of Obstetrics and Gynecology, Tongji Hospital, Tongji Medical College, Huazhong University of Science and Technology, 1095 Jiefang Ave., Wuhan 430030, China. Email: zhangling0709@tjh.tjmu.edu.cn.

Background: Unilateral genital tract obstruction with ipsilateral renal anomaly (UGTOIRA) syndrome is a rare congenital urogenital anomaly, characterized by different combinations of uterine abnormalities, unilateral cervical-vaginal obstruction, and ipsilateral renal abnormalities. Timely and correct diagnosis is critical. In this study, we analyzed the diverse ultrasound image features of UGTOIRA syndrome on genitourinary system segmental sequential ultrasound screening (SSUS) and the accuracy of ultrasonic diagnosis.

Methods: The data from 59 patients with UGTOIRA syndrome over the last decade were analyzed retrospectively, which included ultrasound presentations and diagnoses of abnormalities of the uterus, cervix, and vagina, as well as the conditions associated with the bilateral fallopian tubes, ovaries, pelvis, kidneys and ureters, bladder, and urethra.

Results: All 59 patients (100%) were found to have ipsilateral renal agenesis, and the diagnostic accuracy of ultrasound was 100%. The uterus was correctively diagnosed as complete bicorporal uterus in 42 cases (71.2%), bicorporal septate uterus in 7 cases (11.9%), complete uterus septate in 8 cases (13.6%), partial uterus septate in 1 case (1.7%), and unilateral isthmus atresia in 1 case (1.7%). The cervix was correctively diagnosed as septate cervix in 28 cases (47.5%), double cervix in 17 cases (28.8%), unilateral small cervix in 5 cases (8.5%), unilateral obliterated cervical orifice in 5 cases (8.5%), partial development of the unilateral cervix with a blind end in 3 cases (5.1%), and unilateral completely undeveloped cervix appearing as a normal cervix in 1 case (1.7%). The vagina was correctively diagnosed as oblique vaginal septum (OVS) in 45 cases (76.3%), and normal vagina in 13 cases (22.0%) via preoperative ultrasound. In 1 case (1/59, 1.7%) of high OVS with ipsilateral obliterated external cervical orifice, the OVS was missed by preoperative ultrasound. The ultrasound diagnostic accuracy rates of uterine malformation, cervical malformation, vaginal malformation, hematoma location and volume, uterine communication, and cervical communication were respectively 100%, 100%, 98.3%, 100%, 100%, and 100%. The ultrasonic detection rate for a hole on the OVS was 0%, and the missed diagnosis rate was 100%.

Conclusions: SSUS can be used to accurately evaluate uterine, cervical, and vaginal malformation, obstruction site, location and volume of keratocele, cervical or uterine communication, and ovarian endometriosis cyst in patients with UGTOIRA syndrome and ipsilateral urinary system malformation.

[^] ORCID: Ling Zhang, 0000-0002-7811-2585; Rong Liu, 0000-0002-6094-536X; Shuangmei Ye, 0000-0002-2693-734X.

However, ultrasound is unable to identify a hole on the OVS.

Keywords: Uterine malformation; cervical malformation; vaginal malformation; renal agenesis; ultrasonography

Submitted Feb 19, 2023. Accepted for publication Aug 18, 2023. Published online Sep 06, 2023.

doi: 10.21037/qims-23-204

View this article at: <https://dx.doi.org/10.21037/qims-23-204>

Introduction

Unilateral genital tract obstruction with ipsilateral renal anomaly (UGTOIRA) syndrome is a rare congenital urogenital anomaly involving unilateral genital tract obstruction with different uterine malformations and ipsilateral renal agenesis; in the literature, it is also known as Herlyn-Werner-Wunderlich (HWW) syndrome, obstructed hemivagina and ipsilateral renal anomaly (OHVIRA) syndrome, obstructed uterovaginal duplication, oblique vaginal septum (OVS) syndrome, and other terms (1-5). Over the past hundred years, the common clinical manifestations of HWW syndrome have been considered the symptoms of poor blood drainage (periodic lower abdominal pain or blood dripping after menstruation) combined with infection, endometriosis, and pelvic adhesions (1-10). The anatomical abnormalities of most cases are classic double uterine body, double cervix, and OVS; unilateral hematocolpos, hematometra, and hematosalpinx; ovarian endometriosis cyst, pelvic endometriosis; and ipsilateral renal agenesis. However, with the improvement of the resolution of imaging instruments and the accumulation of diagnostic and surgical experience, an increasing number of cases with nonspecific clinical manifestations and non-classical anatomical abnormalities have been recognized (3,4,11-15). In turn, this has promoted a greater appreciation for the abnormal anatomic heterogeneity of the genitourinary system of gynecological imaging diagnostics and surgeons. UGTOIRA syndrome can be characterized by different combinations of uterine abnormalities, unilateral cervical-vaginal obstruction, and ipsilateral renal abnormalities. Most patients with UGTOIRA syndrome need surgical treatment to prevent complications and preserve fertility.

To this end, timely and correct diagnosis is critical. In addition to clinical symptoms and signs, imaging examination, mainly ultrasound and magnetic resonance imaging (MRI), is crucial for diagnosis. Pelvic ultrasonography is the first choice for imaging examination in most hospitals in China and several other countries.

However, owing to an incomplete understanding of the diverse ultrasonic features of this complex syndrome, many ultrasound clinicians misdiagnose or delay the diagnosis of UGTOIRA syndrome. Thus far, the literature on the ultrasonic characteristics of UGTOIRA syndrome has been limited to case reports or small series (16,17).

In this paper, we propose the segmental sequential ultrasound screening (SSUS) process for UGTOIRA syndrome and report the imaging features and diagnosis (and the specific frequencies) of patients with UGTOIRA syndrome on SSUS, as well as their correlation to clinical and surgical features. Through case analysis and experience summary, we aim to continuously improve the ability of ultrasound to accurately diagnose different anatomical variations of UGTOIRA syndrome and emphasize the guiding significance of SSUS in clinical management, surgical strategy formulation, and surgical effect evaluation.

Methods

Study design

This study involved a retrospective and descriptive analysis of data collected during routine medical diagnosis and treatment of UGTOIRA syndrome, which included pre- and post-operative ultrasonic images and reports from the ultrasonic reporting system, diagnostic instruments, storage equipment, as well as intraoperative findings and discharge diagnoses; individual consent for this retrospective analysis was waived. This study was conducted following the Declaration of Helsinki (as revised in 2013) and was approved by the Medical Ethics Committee of Tongji Hospital Affiliated to Tongji Medical College of Huazhong University of Science and Technology (No. TJ-IRB20220917).

Study population

The included cases were patients with UGTOIRA syndrome who were treated in the Department of Obstetrics and

Gynecology of Tongji Hospital, affiliated with Tongji Medical College of Huazhong University of Science and Technology, from July 2012 to August 2022. Inclusion criteria included those undergoing surgical treatment in our hospital; genitourinary system SSUS performed before the operation; abnormalities of the uterus, cervix, and vagina, as well as the conditions of the bilateral fallopian tubes, ovaries, and pelvis being accurately diagnosed during the operation via laparoscopic exploration or laparotomy, hysteroscopy, or gynecological examination with or without pathologic diagnosis; and at least 1 follow-up visit to the hospital. All cases that did not meet all of the above criteria were excluded from this study.

Ultrasonic examination method, diagnostic process of SSUS, and ultrasound data collection in routine ultrasound diagnosis

All examinations were performed by an experienced, fulltime gynecologic ultrasound clinician. The ultrasound instruments used included the Voluson 730, 730 Pro, S8, S8 Pro, E6, E8, or E10 with the RAB2-5D, RAB4-8RS, RAB6-D, RAB4-8D, or RM6C 3D/4D convex volume probe and the RIC5-9W-RS or RIC5-9-D endo cavity volume probe (GE HealthCare). The examination process combined transabdominal, transperineal, transvaginal, or transrectal ultrasound scanning (bidimensional and tridimensional). For patients without a history of sexual activity, it is recommended that they properly fill their bladder, undergo transabdominal ultrasound examination with an abdominal volume ultrasound probe in a gynecological examination mode. The long axis of the uterus was examined on longitudinal section first with a continuous parallel sliding probe from the right edge to the left edge of the uterus. The external contour and endometrial morphology of the uterus were observed, and the dynamic images and the median sagittal section of the uterus were retained. The probe was slid down the sagittal section to observe the vaginal gas line on one side and then to the opposite side to observe the hematocoe in the posterior space of the OVS. After the observation of sagittal section, the probe was rotated 90° counterclockwise, and the transverse section was continuously scanned from top to bottom to observe the external contour of the uterus, uterine cavity shape, cervical external contour, cervical canal, unilateral gas line, OVS, and hematocoe in the posterior space of the OVS. The dynamic image and maximum transverse sections of the uterus, cervix, and

vagina were retained. After the examination of uterine body, cervix, and vagina, the probe was slowly tilted and slid from the uterine angle to the adnexal area, and the probe was rotated to dynamically scan the ovaries and fallopian tubes, with the dynamic images and maximum sagittal section and transverse section of the ovaries and fallopian tubes being retained. The probe was then slid to continuously scan the pelvic cavity in a large range to observe pelvic hematocoe, inflammation, adhesion, and endometriosis. Finally, the abdominal renal examination mode was used in conjunction with an abdominal volume ultrasound probe to scan the bilateral renal area, the fallopian tube running area, the bladder, and urethra. The connection between the ureteral vestigial cyst and lower reproductive tract can be observed by transvaginal or transrectal ultrasound. If the patient's abdominal wall is too thick or some details of the transabdominal ultrasound are uncertain, the patient is advised to empty their bladder and undergo a transrectal ultrasound examination with an intravaginal probe to obtain a clear image or to supplement the required details. For patients with a history of sexual activity, it is recommended that they empty their bladder and undergo transvaginal ultrasound via an intravaginal probe to obtain clear sagittal and transverse section information. All patients with OVS are recommended to undergo transperineal ultrasound examination with an abdominal ultrasound probe to observe the distance from the lower end of the OVS to the vaginal vestibule. During the transabdominal, transvaginal, or transrectal examination of uterus and vagina, the 3-dimensional Render mode should be activated to obtain the volume data and reconstruct the coronal section image after the completion of 2-dimensional gray-scale ultrasound.

Figure 1 shows the flowchart of the SSUS operation including for the uterine body, cervix, vagina, fallopian tube, ovary, pelvic cavity, bilateral kidneys and ureters, bladder, and urethra. First, the central area behind the bladder (from top to bottom) was scanned, followed by the uterine body. The external uterine profile and shape of the uterine cavity were observed to judge whether there was a complete bicorporal uterus, partial bicorporal uterus, bicorporal septate uterus, complete uterus septate, or partial uterus septate with or without communication and with or without hematometra. The amount of accumulated blood was measured, and then the cervix was scanned to observe the number of cervices and the presence or absence of cervical obstruction, with or without communication, and the location and size of the fistula. The amount of accumulated blood in the cervical canal of the atresia side was measured;

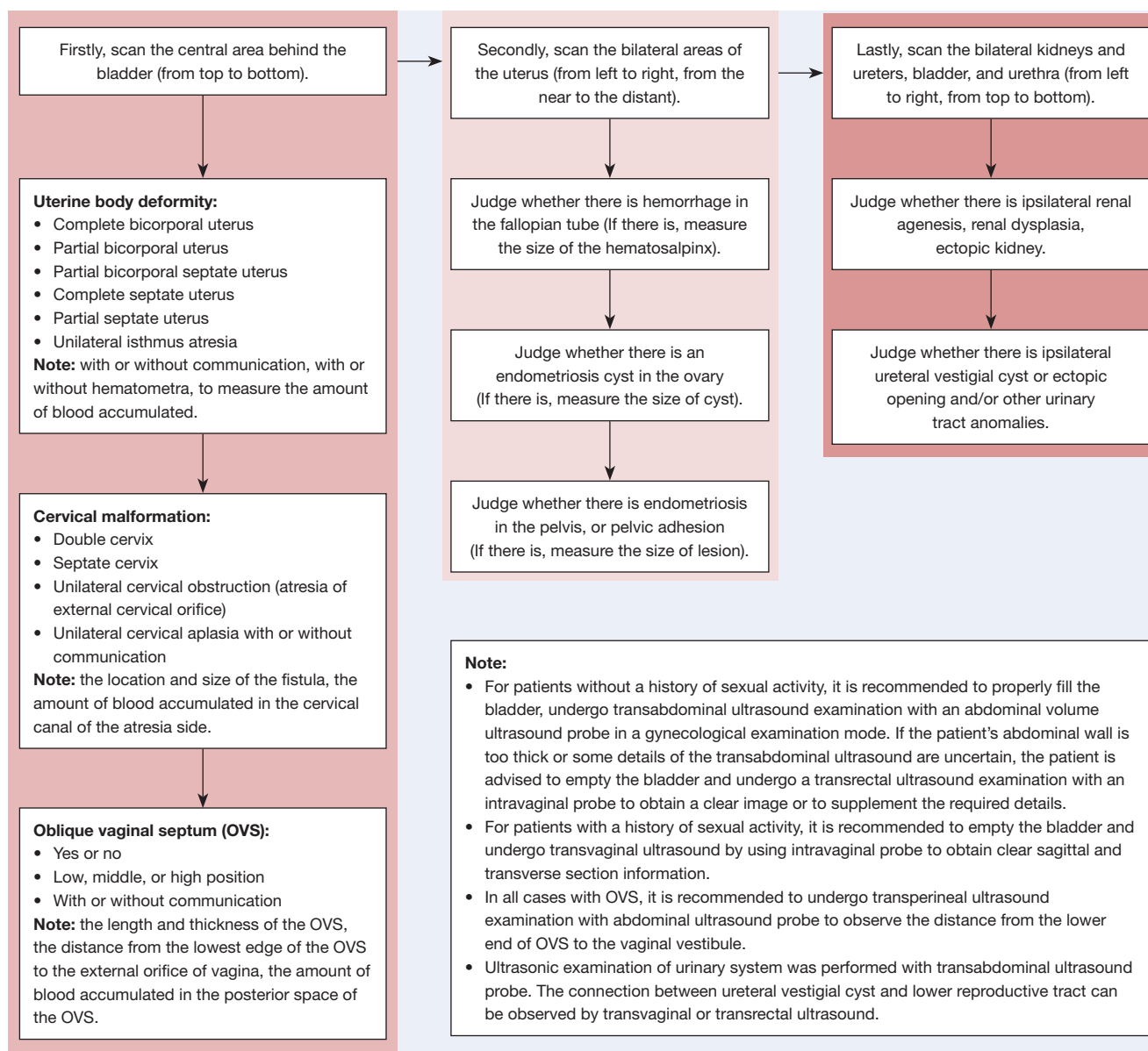


Figure 1 Flowchart of SSUS for UGTOIRA syndrome. SSUS, segmental sequential ultrasound screening; UGTOIRA, unilateral genital tract obstruction with ipsilateral renal anomaly.

then, the vagina was scanned to observe the presence or absence of the OVS, with or without communication, and to measure the length and thickness of the OVS, the distance from the lowest edge of the OVS to the external orifice of vagina, and the amount of blood accumulated in the posterior space of the OVS. Second, the bilateral areas of the uterus (from left to right, from the near to the distant) were scanned to judge whether there was a

hemorrhage in the fallopian tube, an endometriosis cyst in the ovary, endometriosis in the pelvis, or pelvic adhesion, with the size of each lesion being measured. Finally, the bilateral kidneys and ureters, bladder, and urethra (from left to right and from top to bottom) were scanned to screen for renal agenesis, dysplasia, ectopic ureteral vestigial cyst or ectopic opening, and/or other urinary tract anomalies.

Ultrasonic diagnostic criteria of UGTOIRA syndrome on SSUS

Uterine, cervical, and vaginal malformation and obstructive site

Uterine, cervical, and vaginal malformations were classified based on the European Society of Human Reproduction and Embryology/European Society for Gynaecological Endoscopy (ESHRE/ESGE) consensus on the classification of female genital tract congenital anomalies (18).

The uterine body malformations of UGTOIRA syndrome include the following six conditions: (I) partial bicorporal (U3a), presenting as an external fundal indentation partly dividing the uterine corpus above the level of the cervix; (II) complete bicorporal (U3b), presenting as two completely separated corpora, with a deep external fundal indentation to the level of the cervix; (III) bicorporal septate (U3c), presenting as the depth of the midline fundal indentation exceeding the uterine wall thickness by 150%; (IV) partial septate (U2a), presenting as the a septum partly dividing the uterine cavity above the level of the internal cervical orifice with a normal fundal outline; (V) complete septate (U2b), presenting as a septum fully dividing the uterine cavity from the fundal of uterine cavity to the level of the internal cervical orifice with a normal fundal outline; and (VI) unilateral isthmus atresia (U4a).

The cervix malformations of UGTOIRA syndrome include the following six conditions: (I) completely undeveloped unilateral cervix appearing as a normal cervix (C0); (II) septate cervix (C1), presenting as a normal externally rounded cervix with the presence of a septum; (III) double cervix (C2), presenting as 2 distinct, externally rounded cervixes, which may be either fully divided or partially fused; (IV) unilateral cervix exhibits reduced size without obstruction (C3a); (V) unilateral cervix exhibits atresia of the external orifice (C3b); and (VI) unilateral cervix exhibits partial aplasia (C3c).

The longitudinal obstructing vaginal septum (V2), which is often referred to as OVS in Chinese clinics, refers to the lower end of the vaginal septum being attached to the vaginal lateral wall and the vaginal cavity behind the septum not opening directly to the vaginal vestibule. The diagnostic criteria of low, middle, and high OVS correspond to a distance between the inferior edge of the OVS and the vaginal vestibule of ≤ 3 , >3 – ≤ 6 , and >6 cm, respectively. When the unilateral vagina is completely undeveloped, the vagina appears similar to a normal vagina (V0).

Classification of blood volume at different sites

The blood volume in the genital tract was classified. When the average values of the maximum upper and lower diameters, anterior and posterior diameters, and transverse diameters of the posterior vaginal septum hematocele were less than or equal to 3 cm, this was defined as a small amount of hematocele; when the values were greater than 3 cm and less than or equal to 6 cm, this was defined as a medium amount of hematocele; when the values were greater than 6 cm, this was defined as a large amount of hematocele. The hematocele in the cervical canal and intrauterine cavity was defined as a small amount of hematocele when the maximum anteroposterior diameter of the blood in the median sagittal section area was less than or equal to 1 cm, a medium amount of hematocele when it was greater than 1 cm and less than or equal to 3 cm, and a large amount of hematocele when it was greater than 3 cm. When the maximum transverse diameter of the fallopian tube hematocele was less than or equal to 1 cm, this was defined as a small amount of keratocele; when it was greater than 1 cm and less than or equal to 3 cm, this was defined as a medium amount of hematocele; when it was greater than 3 cm, this was defined as a large amount of hematocele. The hematocele in the pelvic cavity and abdominal cavity was only classified as with or without.

Communication sites

The presence and specific location of communication parts were evaluated. The sites of communication between the left and right genital tracts included (I) the lower part of the uterine cavity; (II) the internal orifice of the cervix; (III) fistula on the cervix septum; (IV) the foramen on the OVS; and (V) ≥ 2 communication sites.

Complications

The presence and size of the uterine endometriosis and ovarian endometriotic cyst were evaluated.

Ipsilateral urinary malformation

The loss and dysplasia of the ipsilateral kidney, a vestigial cyst of the ipsilateral ureter, and ectopic genital tract insertion were determined.

Comprehensive diagnosis and typing of UGTOIRA syndrome

A diagnosis of UGTOIRA syndrome was made based on

the following ultrasonic presentations: (I) uterine body deformity, including U3a, U3b, U3c, U2a, U2b, and U4a, with or without communication; (II) cervical malformation, including C1, C2, C3a, C3b, and C3c, with or without communication; (III) V2, including low, middle, and high OVS, with or without communication; and (IV) ipsilateral renal agenesis or dysplasia.

All cases were classified into five types according to the site of obstruction as follows: (I) type I, defined as vaginal obstruction (V2 and C1/C2) and divided into three subtypes of type I-a (low OVS), type I-b (middle OVS), and type I-c (high OVS); (II) type II, defined as cervicovaginal obstruction, (V2 and C3a/C3b); type II is divided into two subtypes of type II-a (C3aV2) and type II-b (C3bV2); (III) type III, defined as cervical obstruction (C3bV0); (IV) type IV, defined as unilateral partial cervical aplasia (C3cV0); and (V) type V, defined as unilateral isthmus atresia (U4aC0V0).

Clinical data collection

The medical history of patients was obtained from inpatient records, including clinical demographic information, clinical presentation, imaging examination, gynecological examination, management, operation findings, pathologic diagnosis, and follow-up information. SSUS and operation findings were extracted for analysis.

Statistical analyses

The statistical software package SPSS 26.0 (IBM Corp., Armonk, NY, USA) was used for data analysis. The data of classified variables are expressed as number and percentages, and the data of continuous variables represented by medium with quartiles [25%, 75%]. All continuous variables were rounded to an integer, and percentages and ultrasound diagnostic accuracy were calculated to a single decimal place. For multi-row and multi-list analyses, Fisher exact test was used directly. The P value is expressed as 3 decimal places after the decimal point. The difference was statistically significant when the P value <0.05.

Results

A total of 59 cases were eligible for inclusion in this study. All the cases accepted preoperative SSUS and underwent surgical treatment for removal of unilateral genital obstruction. The median age at diagnosis was 15 [12, 23] years, with a range

from 5 to 52 years. The median interval between diagnosis and operation was 0 [0, 0] months, with intervals ranging from 0 to 12 months.

Uterine, cervical, and vaginal malformation and obstructive site

The uterus was diagnosed as complete bicorporal uterus (U3b) in 42 cases (71.2%), bicorporal septate uterus (U3c) in 7 cases (11.9%), complete uterus septate (U2b) in 8 cases (13.6%), partial uterus septate (U2a) in 1 case (1.7%), and unilateral isthmus atresia (U4a) in 1 case (1.7%). No cases were diagnosed as partial bicorporal uterus (U3a). A total of 45 (76.3%) cases had vaginal obstruction without cervical aplasia. Among these cases, 17 (17/45) showed a double cervix with OVS without cervical obstruction (C2V2), and 28 (28/45) showed a septate cervix with OVS without cervical obstruction (C1V2); 13 cases (22.0%) presented cervical obstruction, 5 of whom were associated with ipsilateral vaginal obstruction. The number and incidence of different uterine anomalies in different types and subtypes of UGTOIRA syndrome according to discharge diagnosis are shown in *Figure 2*. The diagnosis of uterine and cervical anomaly with ultrasound was consistent with surgery findings in all cases (59/59, 100%). The diagnosis of vaginal anomaly by ultrasound was in accordance with the surgery findings in 58 cases (58/59, 98.3%). In 1 case (1/59, 1.7%) of vaginal high oblique septum with ipsilateral cervical atresia, the OVS was missed by preoperative ultrasound because there was no blood accumulation behind the OVS.

Location and size of hematocele

Hematocele was found in the posterior space of the OVS (50/59, 84.7%), cervical canal (34/59, 57.6%), uterine cavity (21/59, 35.6%), fallopian tube (13/59, 22.0%), pelvic cavity (1/59, 1.7%), and abdominal cavity (2/59, 3.4%). The numbers of cases of each type and subtype of UGTOIRA syndrome in different hematocele sites and with different blood volumes are shown in the *Table 1*. The difference in the locations and volumes of hematocele in different types of UGTOIRA syndrome subtypes was statistically significant, except for pelvic hematocele and peritoneal hematocele, as these had too few cases. The diagnosis of location and volume of hematocele with ultrasound was in accordance with the surgery findings in all cases (59/59, 100%).

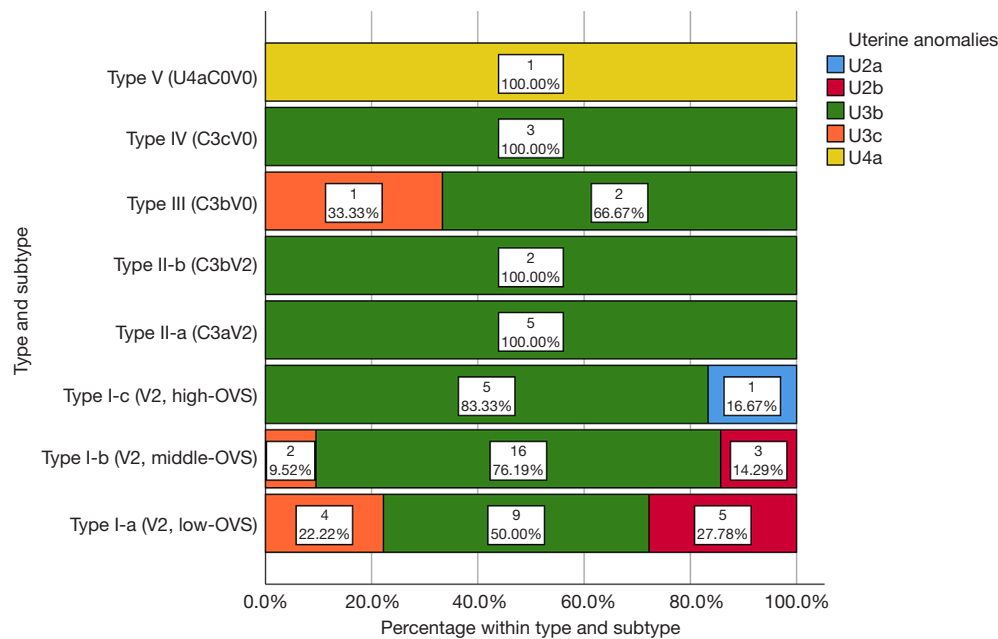


Figure 2 The number and incidence of different uterine anomalies in different types and subtypes of UGTOIRA syndrome (n=59). U2a, partial septate uterus; U2b, complete septate uterus; U3b, complete bicorporal uterus; U3c, bicorporal septate uterus; U4a, unilateral isthmus atresia; C0, completely undeveloped ipsilateral cervix appearing as a normal cervix; V0, completely undeveloped ipsilateral vagina, appearing as a normal vagina; C3c, partial non-development of the unilateral cervix with a blind end; C3b, unilateral obliterated cervical orifice; C3a, unilateral small cervix; V2/OVS, oblique vaginal septum; UGTOIRA, unilateral genital tract obstruction with ipsilateral renal anomaly.

Communication sites

Of the 59 cases, 14 (23.7%) had communication sites identified with preoperative ultrasound and confirmed by surgery, including 1 (1.7%) case of lower uterine cavity communication, 10 cases (16.9%) of internal orifice of cervix communication, and 3 (5.1%) cases of fistula on the cervix septum. A total of 22 (37.3%) cases of foramen on the OVS were missed on ultrasound; among these, there were 2 cases of internal oral communication combined with foramen on the OVS where the internal oral communication was found on preoperative ultrasound, but the foramen on the OVS was missed. There were 25 cases (42.4%) with no perforations found with preoperative ultrasound and surgery. The ultrasound detection rate of communication in the lower segment of the uterine cavity, the internal orifice of the cervix, and the cervical mediastinum was 100%, and the missed diagnosis rate was 0. The ultrasonic detection rate of a hole on the OVS was 0, and the missed diagnosis rate was 100%.

Complications

Two cases of adenomyoma, 2 cases of adenomyoma with an ipsilateral ovarian endometriosis cyst, and 6 cases of an ipsilateral ovarian endometriosis cyst were detected by ultrasonography, all of which were confirmed by surgery. No cases were diagnosed as pelvic endometriosis, genital tract, pelvic inflammation, or pelvic adhesion on preoperative ultrasound. During the operation, 4 cases of pelvic endometriosis, 1 case of colonic endometriosis, 7 cases of genital and pelvic inflammation, and 13 cases of pelvic adhesions were found.

Ipsilateral urinary malformation

During preoperative ultrasound examination, all 59 patients (100%) were found with ipsilateral renal agenesis, and 4 patients (6.8%) were also found with a long and thin tube between the ipsilateral bladder and the vagina and connected to the vagina, which was considered to be an

Table 1 Frequency of cases of each type and subtype of UGTOIRA syndrome in different hematocele sites and with different blood volume (n=59)

Hematocele site	Blood volume	Type and subtype (n)								Total No. (% of all)	P value (chi-squared test)
		Type I (V2, C1/C2)			Type II (V2, C3a/C3b)		Type III (C3bV0)	Type IV (C3cV0)	Type V (U4aC0V0)		
		Type I-a (low OVS)	Type I-b (middle OVS)	Type I-c (high OVS)	Type II-a (C3aV2)	Type II-b (C3bV2)					
Posterior OVS	No	0	0	0	0	2	3	3	1	9 (15.3)	0.000
	Small	2	7	4	3	0	0	0	0	16 (27.1)	
	Medium	6	11	2	0	0	0	0	0	19 (32.2)	
	Large	10	3	0	2	0	0	0	0	15 (25.4)	
Cervical canal	No	7	12	2	3	0	0	0	1	25 (42.4)	0.034
	Small	4	3	1	2	0	3	3	0	16 (27.1)	
	Medium	5	3	3	0	0	0	0	0	11 (18.6)	
	Large	2	3	0	0	2	0	0	0	7 (11.9)	
Uterine cavity	No	10	18	5	3	0	1	1	0	38 (64.4)	0.008
	Small	5	1	0	1	0	1	1	0	9 (15.3)	
	Medium	1	2	1	1	0	0	1	0	6 (10.2)	
	Large	2	0	0	0	2	1	0	1	6 (10.2)	
Fallopian tube	No	13	21	5	4	0	2	1	0	46 (78.0)	0.000
	Small	3	0	1	0	0	1	0	0	5 (8.5)	
	Medium	2	0	0	1	2	0	2	0	7 (11.9)	
	Large	0	0	0	0	0	0	0	1	1 (1.7)	
Pelvic cavity	No	17	21	6	5	2	3	3	1	58 (98.3)	0.644
	Yes	1	0	0	0	0	0	0	0	1 (1.7)	
Abdominal cavity	No	18	20	6	5	2	2	3	1	57 (96.6)	0.316
	Yes	0	1	0	0	0	1	0	0	2 (3.4)	

UGTOIRA, unilateral genital tract obstruction with ipsilateral renal anomaly; U4a, unilateral isthmus atresia; C0, completely undeveloped ipsilateral cervix appearing as a normal cervix; C1, septate cervix; C2, double cervix; C3a, unilateral small cervix; C3b, unilateral obliterated cervical orifice; C3c, partial non-development of the unilateral cervix with a blind end; V0, completely undeveloped ipsilateral vagina appearing as a normal vagina; V2/OVS, oblique vaginal septum.

ipsilateral ectopic insertion of a ureteral remnant into the vagina. Left and right genital tract obstruction were found in 29 cases (49.2%) and 30 cases (50.8%), respectively.

Ultrasound image findings of different types and subtypes of UGTOIRA syndrome

Type I (V2, C1/C2)

A total of 45 cases (45/59, 76.3%) were diagnosed with type I UGTOIRA syndrome that had vaginal obstruction without cervical aplasia. Among these, 18 cases (18/45)

were classified as type I-a, 21 cases (21/45) as type I-b, and 6 cases (6/45) as type I-c. The hematocele was mainly located in the posterior cavity of the OVS, cervical canal, and uterine cavity. Cervical dilatation was trumpet-shaped. The difference in blood volume in the same segment of the genital tract between different subtypes was statistically significant.

In cases of type I-a, 5 (5/18) showed complete septate uterus (U2b), septate cervix (C1) and low OVS; 4 cases (4/18) showed complete bicorporal uterus (U3b), septate cervix (C1), and low OVS; 5 cases (5/18) showed complete

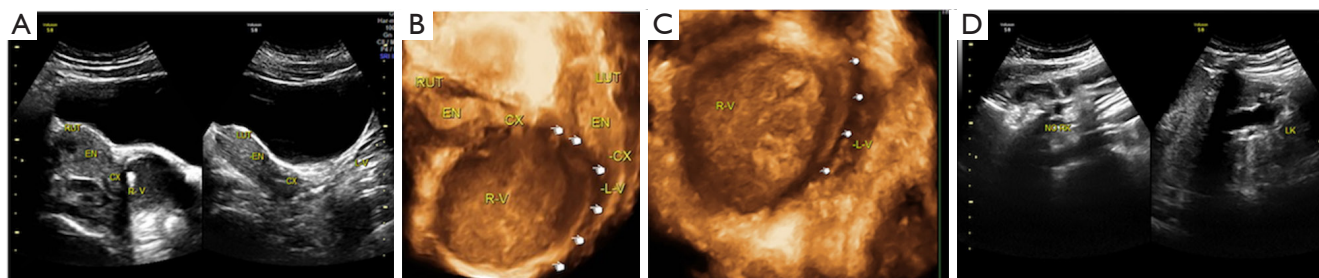


Figure 3 Type I-a UGTOIRA syndrome: U3b-C2-low OVS, complete bicorporal uterus, double cervix without cervical obstruction, with right-low OVS (without communication observed intraoperatively), and right renal agenesis. Sonograms were obtained from a 17-year-old female patient. (A) TAS 2D sagittal pelvic planes demonstrating a normal right uterus, cervix, and a large amount of hematocoele in the posterior space of the OVS (left side of the figure), normal left uterus, cervix, and left vagina (right side of the figure). (B) TAS 3D coronal plane of the demonstrating complete bicorporal uterus, double cervix, and right-low OVS with a large amount of hematocoele in the posterior space of the OVS (the hand arrows indicate the OVS). (C) TAS 3D coronal plane of the vagina under stereoscopy demonstrating the right-low OVS with a large amount of hematocoele in the posterior space of the OVS, without communication (the hand arrows indicate the OVS). (D) TAS 2D sagittal planes identifying the absence of the right kidney (NO RK; left side of the figure) and a normal left kidney (LK; right side of the figure). RUT, right uterus; EN, endometrium; CX, cervix; R-V, right vagina; LUT, left uterus; L-V, left vagina; RK, right kidney; LK, left kidney; UGTOIRA, unilateral genital tract obstruction with ipsilateral renal anomaly; OVS, oblique vaginal septum; TAS, transabdominal sonography; 2D, 2-dimensional; 3D, 3-dimensional.

bicorporal uterus (U3b), double cervix (C2), and low OVS (Figure 3); and 4 cases (4/18) showed bicorporal septate uterus (U3c), septate cervix (C1) and low OVS (Figure 4). In this subtype of cases, there was often more blood in the posterior cavity of the OVS and less blood in the cervical canal and uterine cavity. In 4 cases (4/18), there was communication at the internal orifice of cervix; in 5 cases (5/18), a hole was found in the OVS during the operation that had not been found on preoperative ultrasound. One patient (1/18) was found with adenomyoma of the affected side.

Of the type I-b cases, 2 (3/21) showed complete septate uterus (U2b), septate cervix (C1) and middle OVS (Figure 5); seven (7/21) showed complete bicorporal uterus (U3b), septate cervix (C1), and middle OVS (Figure 6); 9 (9/21) showed complete bicorporal uterus (U3b), double cervix (C2), and middle OVS (Figure 7); and 2 (2/21) showed bicorporal septate uterus (U3c), septate cervix (C1), and middle OVS. Most cases of this subtype had a moderate amount of blood accumulation in the posterior cavity of the OVS and in the cervical canal and uterine cavity, and 4 cases (4/21) had communication at the internal orifice of cervix. In 14 cases (14/21), a hole was found in the OVS during the operation, but it was not found on preoperative ultrasound, and 2 of these cases of combined cervical internal orifice communication were detected with preoperative ultrasound.

One patient (1/21) had adenomyoma on the affected side, and one patient (1/21) had an ovarian endometriosis cyst on the affected side.

In type I-c cases, 1 (1/6) showed a partial septate uterus (U2a), septate cervix (C1), and high OVS (Figure 8); 2 (2/6) showed a complete bicorporal uterus (U3b), septate cervix (C1), and high OVS (Figure 9); and 3 (3/6) showed a complete bicorporal uterus (U3b), double cervix (C2), and high OVS. In this subtype, there was less blood in the posterior cavity of the OVS, more blood in the cervical canal and uterine cavity, and even a small amount of blood in the fallopian tube. One case (1/6) had communication at the internal orifice of the cervix, and one case (1/6) had communication at the lower part of the uterine cavity. In 2 cases (2/6), a hole was found in the OVS during the operation, but it was not found on preoperative ultrasound.

Type II (V2, C3a/C3b)

Seven cases (7/59, 11.9%) were diagnosed as type II UGTOIRA syndrome, with vaginal obstruction and cervical aplasia. Among these cases, 5 (5/7) were classified as type II-a and 2 (2/7) as type II-b.

Moreover, 5 cases of type II-a had a complete bicorporal uterus (U3b), ipsilateral small cervix (C3a), and high OVS. There was a lower amount of hematocoele in the posterior space of the OVS and cervical canal, a greater amount of

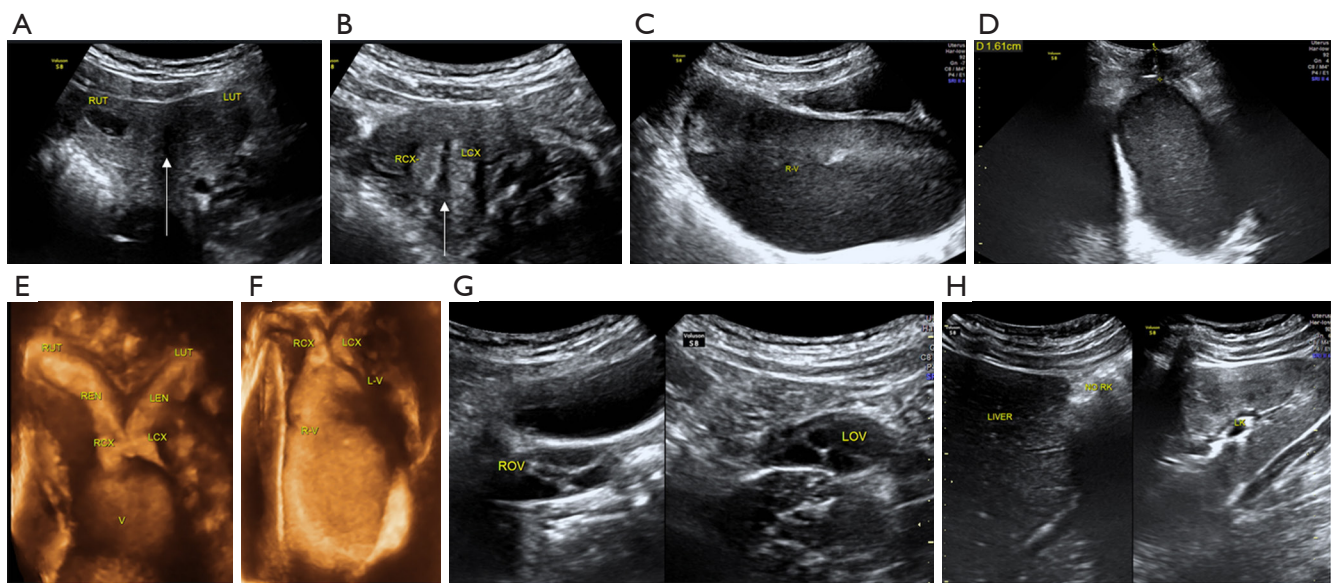


Figure 4 Type I-a UGTOIRA syndrome: U3c-C1-low OVS, bicorporal septate uterus, septate cervix without cervical obstruction, with right-low OVS (without communication observed intraoperatively), and right renal agenesis. Sonograms were obtained from an 11-year-old female patient. (A) TAS 2D coronal plane of the uterus demonstrating right hematometra and normal left uterus (the arrow indicates the uterine septum). (B) TAS 2D coronal plane of the cervix demonstrating the cervical septum (the arrow indicates the cervical septum). (C) TAS 2D sagittal plane of the right cervix-vagina demonstrating a large amount of hematocele in the posterior space of the OVS. (D) TPS 2D sagittal section of the perineum demonstrating that the lower edge of the right vaginal hematocele is 1.6 cm from the perineum. (E) TAS 3D coronal plane of the uterus-cervix-vagina under stereoscopy demonstrating the bicorporal septate uterus, septate cervix, and right-low OVS with a large amount of hematocele in the posterior space of the OVS. (F) TAS 3D coronal plane of the cervix-vagina under stereoscopy demonstrating the bicorporal septate cervix and right-low OVS with a large amount of hematocele in the posterior space of the OVS. (G) TAS 2D ovarian sagittal planes demonstrating both normal ovaries. (H) TAS 2D sagittal planes identifying the absence of the right kidney (NO RK; left side of the figure) and a normal left kidney (LK, right side of the figure). RUT, right uterus; LUT, left uterus; RCX, right cervix; LCX, left cervix; R-V, right vagina; REN, right endometrium; LEN, left endometrium; V, vagina; L-V, left vagina; ROV, right ovary; LOV, left ovary; RK, right kidney; LK, left kidney; UGTOIRA, unilateral genital tract obstruction with ipsilateral renal anomaly; OVS, oblique vaginal septum; TAS, transabdominal sonography; TPS, transperineal sonography; 2D, 2-dimensional; 3D, 3-dimensional; RCY, right ovarian cyst.

hematocele in the uterine cavity, and a moderate amount of hematocele in the fallopian tube. The cervix was tubular dilated. One case (1/5) had a fistula on the cervical septum. In one case (1/5), a hole was found in the OVS during the operation, but it was not found on preoperative ultrasound. One patient (1/5) had an ovarian endometriosis cyst on the affected side, and one patient (1/5) had adenomyoma and an ovarian endometriosis cyst on the affected side. In the latter case, pelvic endometriosis was also found during the operation.

Two cases of type II-b both had a complete bicorporal uterus (U3b), ipsilateral obliterated cervical orifice (C3b), and high OVS (Figure 10). One was misdiagnosed as type III because the high OVS was overlooked owing to

the lack of hematocele behind the high OVS. There was no hematocele in the posterior cavity of the OVS, but a greater amount of hematocele was detected in the cervical canal, uterine cavity, and fallopian tube. The cervix that showed obvious dilation of the cervical canal and atresia of the external cervix appeared as an inverted cone. No communication was found with ultrasound or surgery in 2 cases.

Type III (V0C3b)

Three cases (3/59, 5.1%) were diagnosed as type III UGTOIRA syndrome, which presented a unilateral obliterated cervical orifice (C3b) and a completely undeveloped ipsilateral vagina that appeared similar to a

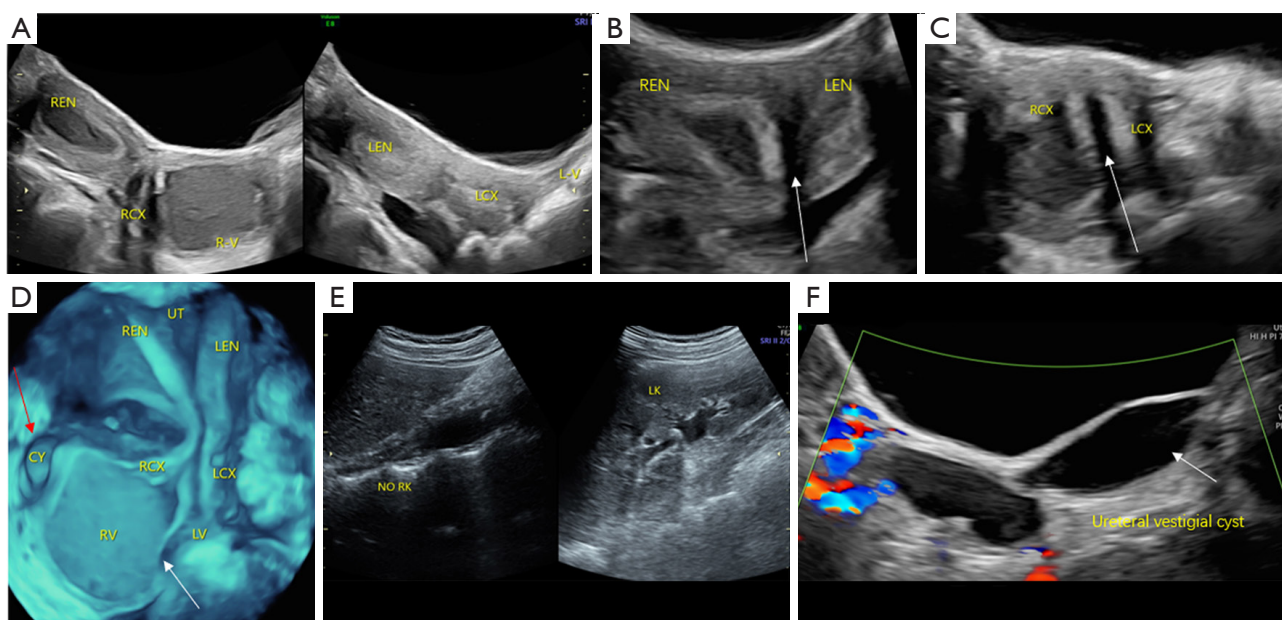


Figure 5 Type I-b UGTOIRA syndrome: U2b-C1-middle OVS, complete septal uterus, septate cervix without cervical obstruction, with right-middle OVS (with a foramen on the OVS observed intraoperatively), and right renal agenesis with right ureteral vestigial cyst. Sonograms were obtained from a 13-year-old female patient. (A) TAS 2D sagittal pelvic planes demonstrating a hemorrhage in the right uterine cavity, cervical canal and the posterior space of the OVS (left side of the figure), normal left uterus, cervix, and left vagina (right side of the figure). (B) TAS 2D coronal section of the uterus demonstrating complete septal uterus (the arrow indicates the septate). (C) TAS 2D cross-section of the cervix demonstrating a septate cervix (the arrow indicates the septate). (D) TAS 3D coronal plane of the uterus-cervix-vagina under stereoscopy demonstrating the complete septal uterus, septate cervix, middle OVS with a medium amount of hematocele in the posterior space of the OVS (the white arrow indicates the OVS), and a ureteral vestigial cyst (the red arrow indicates the cyst), which connected with the right wall of the vaginal vault. (E) TAS 2D sagittal planes identifying the absence of the right kidney (NO RK; left side of the figure) and a normal left kidney (LK; right side of the figure). (F) TAS 2D sagittal plane demonstrating a ureteral vestigial cyst that connected with the trigone of the bladder and the right wall of the vaginal vault (the arrow indicates the ureteral vestigial cyst). REN, right endometrium; RCX, right cervix; RV, right vagina; LCX, left cervix; LV, left vagina; LEN, left endometrium; UT, uterus; CY, cyst; RK, right kidney; LK, left kidney; UGTOIRA, unilateral genital tract obstruction with ipsilateral renal anomaly; OVS, oblique vaginal septum; TAS, transabdominal sonography; 2D, 2-dimensional; 3D, 3-dimensional.

normal vagina (V0). The uterine malformations of 2 cases (2/3) included 1 case of complete bicorporal uterus (U3b) and 1 (1/3) case of bicorporal septate uterus (U3c) (Figure 11). Hemorrhages in this type of case were mainly located in the cervical canal and uterine cavity. The cervix, with an obvious dilation of the cervical canal and atresia of the external cervix, had an inverted cone appearance. One case (1/3) had communication at the internal orifice of cervix, and one case (1/3) had a fistula on the cervical septum. Two patients (2/3) were found with an ovarian endometriosis cyst on the affected side. Pelvic endometriosis was also found in 1 of the 2 patients during the operation.

Type IV (V0C3c)

Three cases (3/59, 5.1%) were diagnosed as type IV UGTOIRA syndrome, which manifest as partial development of a unilateral cervix with a blind end (C3c) and a completely undeveloped ipsilateral vagina that appeared similar to a normal vagina (V0). The uterine malformations of these 3 cases appeared as a complete bicorporal uterus (U3b) (Figure 12). In this type of case, the hematocele was mainly located the uterine cavity and fallopian tube, and the dysplastic cervical tube had a lower amount of hematocele. One case (1/3) had a fistula on the cervical septum. One patient (1/3) had an ovarian

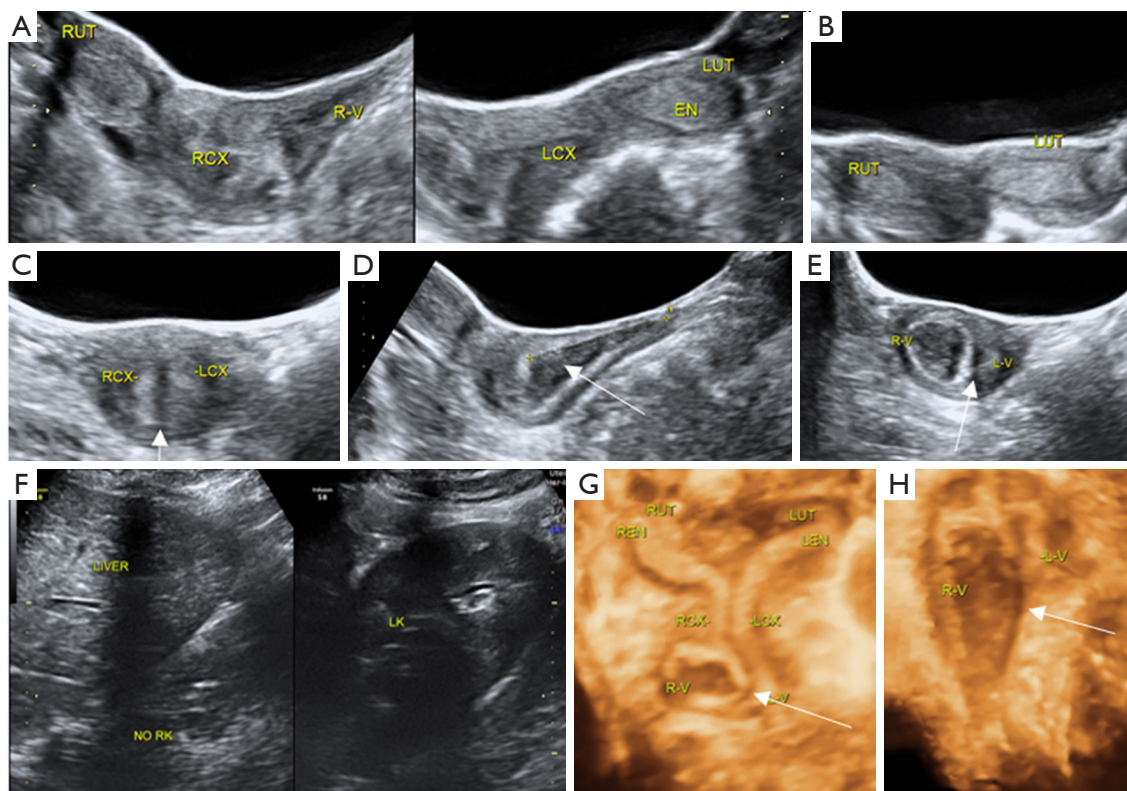


Figure 6 Type I-b UGTOIRA syndrome: U3b-C1-middle OVS, complete bicorporal uterus, septate cervix without cervical obstruction, with right-middle OVS (with a foramen on OVS observed intraoperatively), and right renal agenesis. Sonograms were obtained from a 14-year-old female patient. (A) TAS 2D sagittal pelvic planes demonstrating a normal right uterus and cervix, a small amount of hematocele in the posterior space of the OVS (left side of the figure), and a normal left uterus, cervix, and left vagina (right side of the figure). (B) TAS 2D cross-section of the uterus demonstrating a complete bicorporal uterus. (C) TAS 2D cross-section of the cervix demonstrating a septate cervix (the arrow indicates the septate). (D) TAS 2D sagittal plane of the right cervix-vagina demonstrating a small amount of hematocele in the posterior space of the OVS (the arrow indicates the blood accumulation). (E) TAS 2D cross-section of the middle part of the vagina demonstrating OVS with a small amount of hematocele in the posterior space of the OVS (the arrow indicates the OVS). (F) TAS 2D sagittal planes identifying the absence of the right kidney (NO RK; left side of the figure) and a normal left kidney (LK; right side of the figure). (G) TAS 3D coronal plane of the uterus-cervix-vagina under stereoscopy demonstrating a complete bicorporal uterus, septate cervix, and middle OVS with a small amount of hematocele in the posterior space of the OVS (the arrow indicates the OVS). (H) TRS 3D coronal plane of the cervix-vagina under stereoscopy demonstrating the septate cervix and OVS with a small amount of hematocele in the posterior space of the OVS (the arrow indicates the OVS). RUT, right uterus; RCX, right cervix; R-V, right vagina; LCX, left cervix; LUT, left uterus; EN, endometrium; L-V, left vagina; RK, right kidney; LK, left kidney; UGTOIRA, unilateral genital tract obstruction with ipsilateral renal anomaly; OVS, oblique vaginal septum; TAS, transabdominal sonography; 2D, 2-dimensional; 3D, 3-dimensional; TRS, transrectal sonography.

endometriosis cyst on the affected side, one patient (1/3) had adenomyoma and an ovarian endometriosis cyst on the affected side, and the third patient (1/3) was found to have pelvic endometriosis during the operation.

Type V (V0C0U4a)

One case (1/59, 1.7%) was diagnosed with type V

UGTOIRA syndrome, which showed a unilateral isthmus atresia (U4a), a completely undeveloped ipsilateral cervix that appeared similar to a normal cervix (C0), and a completely undeveloped ipsilateral vagina that appeared similar to a normal vagina (V0) (Figure 13). Hemorrhage in this type of case was mainly located in the uterine cavity and fallopian tube of the rudimentary horn. The patient had an

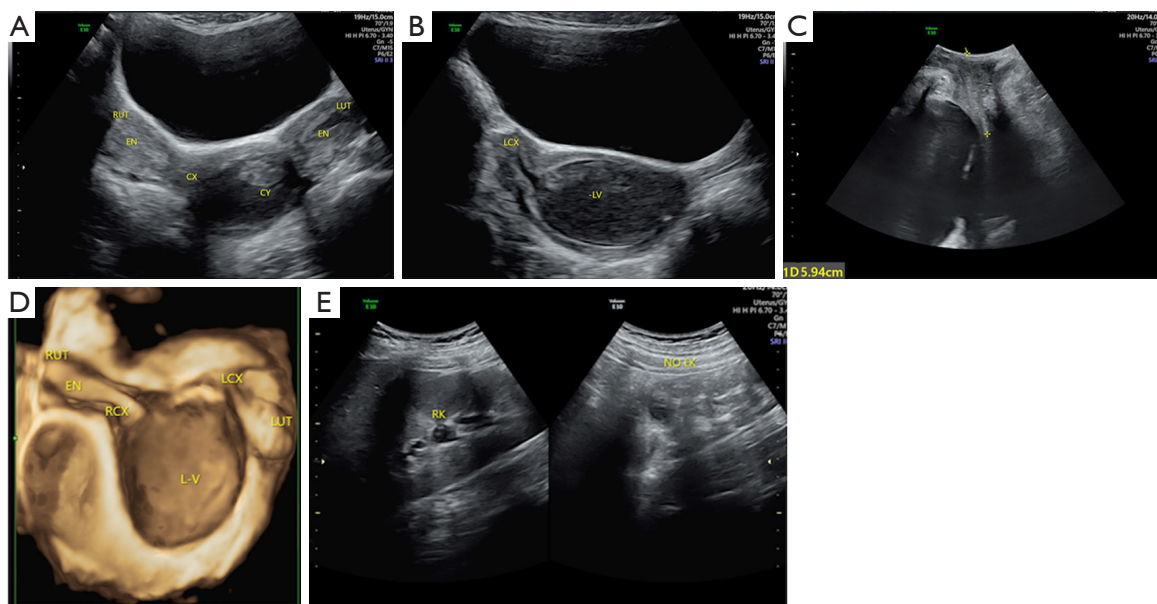


Figure 7 Type I-b UGTOIRA syndrome: U3b-C2-middle OVS, complete bicorporal uterus, double cervix without cervical obstruction, with left middle OVS (without communication observed intraoperatively), and left renal agenesis. Sonograms were obtained from a 12-year-old female patient. (A) TAS 2D coronal plane demonstrating the right normal uterus, cervix, and vagina, and left normal uterus, cervix with keratocele, and middle OVS with a large amount of hematocele in the posterior space of the OVS. (B) TAS 2D sagittal plane of the left uterus-cervix-vagina demonstrating a small amount of hematocele in the left uterine cavity and cervical canal, and a large amount of hematocele in the posterior space of the OVS. (C) TPS 2D sagittal section of the perineum demonstrating that the lower edge of the left vaginal hematocele is 5.9 cm from the perineum. (D) TAS 3D coronal plane of the uterus-cervix-vagina under stereoscopy demonstrating a complete bicorporal uterus, double cervix, and the left middle OVS with a large amount of hematocele in the posterior space of the OVS. (E) TAS 2D sagittal planes identifying the absence of the left kidney (NO LK; right side of the figure) and a right normal kidney (RK; left side of the figure). RUT, right uterus; EN, endometrium; CX, cervix; CY, cyst; LUT, left uterus; LCX, left cervix; LV, left vagina; RCX, right cervix; RK, right kidney; LK, left kidney; UGTOIRA, unilateral genital tract obstruction with ipsilateral renal anomaly; OVS, oblique vaginal septum; TAS, transabdominal sonography; 2D, 2-dimensional; 3D, 3-dimensional; TPS, transperineal sonography.

ovarian endometriosis cyst on the affected side, and pelvic endometriosis was also found during operation.

Discussion

The present study provided a detailed description of the SSUS ultrasonographic features for the genitourinary anatomical variations in UGTOIRA syndrome, in which the descriptions of reproductive tract malformations were consistent with the ESHRE/ESGE consensus on the classification of female genital tract congenital anomalies (18). The frequency of the anatomical variation of each segment of the genital tract was also given in detail. It is obvious from the present study that UGTOIRA syndrome can be characterized by different combinations of uterine body abnormalities, cervical abnormalities without or with

unilateral cervical aplasia and/or vaginal obstruction, and ipsilateral renal abnormalities.

The site of obstruction and the development of the ipsilateral cervix are the key factors in determining the surgical approach and surgical plan, which must be evaluated in detail before operation. When the obstruction was in the vagina, direct ultrasound signs included the position of the OVS (low, middle, or high) and the development of the ipsilateral cervix. Indirect ultrasound signs included bleeding behind the vaginal septum, ipsilateral cervical hemorrhage, uterine hemorrhage, fallopian tube hemorrhage, and ipsilateral kidney abnormalities, and attempts were made to describe the communication. Nearly the entire ipsilateral cervix of the middle OVS and low OVS developed well, and the hemorrhage mainly accumulated in the posterior space of the OVS. The operation mainly involved a complete

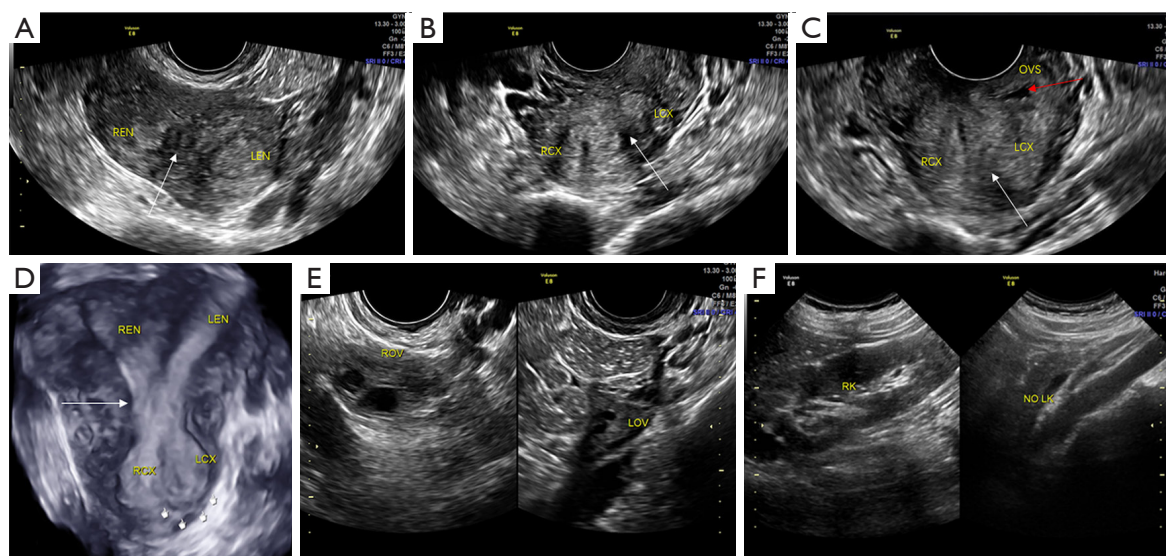


Figure 8 Type I-c UGTOIRA syndrome: U2a-C1-high OVS, partial septate uterus, septate cervix, with left-high OVS, with communication between the left and right lower part of the uterine cavity, and left renal agenesis. Sonograms were obtained from a 24-year-old female patient. (A) TVS 2D uterine cross plane demonstrating a partial septate uterus (the arrow indicates the uterine septate). (B) TVS 2D cross-section of the cervix demonstrating the cervical septate (the arrow indicates the cervical septate). (C) TVS 2D coronal plane of the cervix demonstrating the cervical septate and left-high OVS with a small amount of hematocele in the posterior space of the OVS (the white arrow indicates the cervical septate; the red arrow indicates the hematocele). (D) TVS 3D coronal plane of the uterus-cervix-vagina under stereoscopy demonstrating the partial septate uterus and septal cervix with left-high OVS and a small amount of hematocele filled in the posterior space of the OVS (the arrow indicates the OVS). (E) TVS 2D ovarian sagittal planes demonstrating both normal ovaries. (F) TAS 2D sagittal planes identifying the absence of the left kidney (NO LK; right side of the figure) and a normal right kidney (RK; left side of the figure). REN, right endometrium; LEN, left endometrium; RCX, right cervix; LCX, left cervix; OVS, oblique vaginal septum; ROV, right ovary; LOV, left ovary; RK, right kidney; LK, left kidney; UGTOIRA, unilateral genital tract obstruction with ipsilateral renal anomaly; TVS, transvaginal sonography; TAS, transabdominal sonography; 2D, 2-dimensional; 3D, 3-dimensional.

resection of the OVS. More than half of the cases of high OVS were associated with ipsilateral cervical dysplasia, so in addition to the complete removal of the OVS, cervicoplasty or ipsilateral hysterectomy was performed according to the development of the cervix. When the obstruction site was in the unilateral cervix, the direct ultrasound signs included unilateral obliterated cervical orifice or unilateral partial cervical aplasia with a blind end. Indirect ultrasound signs included ipsilateral cervical hemorrhage, uterine hemorrhage, and fallopian tubal hemorrhage. Ipsilateral hysterectomy was performed for patients with unilateral partial cervical aplasia. Cervicoplasty was feasible when only the external orifice of the cervix was atresic. When the obstruction was in the unilateral isthmus, direct ultrasound signs included unilateral obliterated isthmus with a completely undeveloped ipsilateral cervix that appeared similar to a normal cervix. Indirect ultrasound signs

included ipsilateral uterine hemorrhage and fallopian tubal hemorrhage. Ipsilateral hysterectomy could be considered a feasible therapeutic option. Ultrasound may miss the diagnosis of the OVS when the unilateral obliterated cervical orifice is associated with high OVS and there is no effusion behind the vaginal septum.

The communication between the obstructive side and the contralateral side directly affects the location of hemorrhage, the amount of blood accumulation, the difference in clinical symptoms, the age of seeking medical treatment, and the choice of operation time, thus guiding the surgical approach. According to a clinical study, communicative UGTOIRA syndrome is more common (75%) than is non-communicative UGTOIRA syndrome (25%), with non-communicative UGTOIRA syndrome occurring earlier (13). In our study, 34 cases (57.6%) were surgically found to have communication sites. The ultrasound detection rate

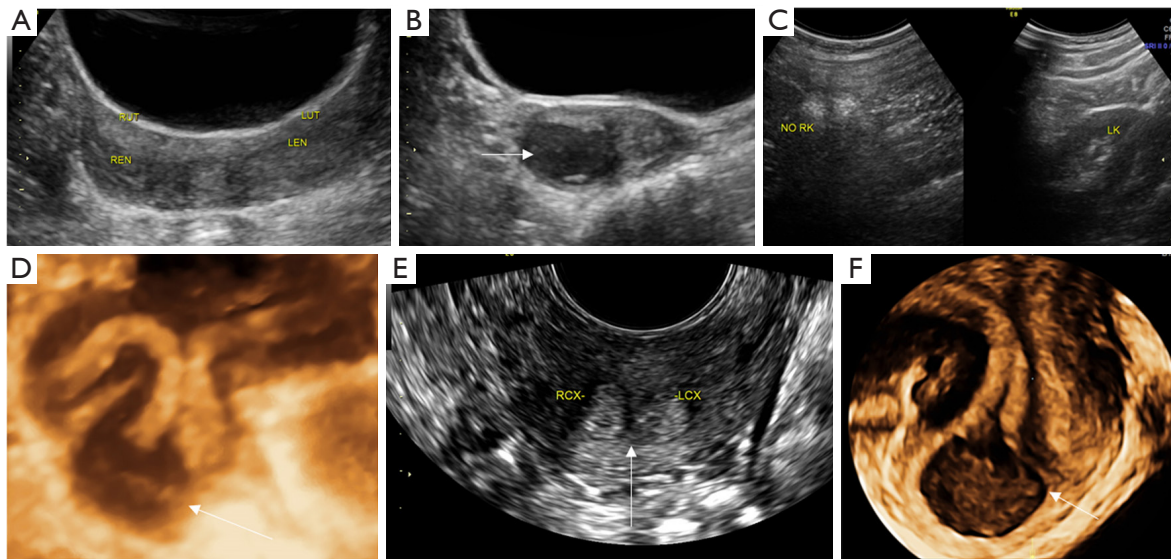


Figure 9 Type I-c UGTOIRA syndrome: U3b-C1-high OVS, complete bicorporal uterus, septate cervix without cervical obstruction, with right-high OVS (with a foramen on the OVS observed intraoperatively), and right renal agenesis. Sonograms were obtained from a 17-year-old female patient. (A) TAS 2D coronal pelvic plane demonstrating the complete bicorporal uterus and septate cervix. (B) TAS 2D cross-section of the lower part of the cervix demonstrating OVS with a small amount of hematocoele in the posterior space of the OVS (the arrow indicates the blood accumulation). (C) TAS 2D sagittal planes identifying the absence of the right kidney (NO RK; left side of the figure) and a normal left kidney (LK; right side of the figure). (D) TAS 3D coronal plane of the uterus-cervix-vagina under stereoscopy demonstrating the complete bicorporal uterus, septate cervix, and high OVS with a small amount of hematocoele in the posterior space of the OVS (the arrow indicates the OVS). (E) TRS 2D cross-section of the cervix demonstrating the cervical septate (the arrow indicates the cervical septate). (F) TRS 3D coronal planes of the cervix-vagina under stereoscopy demonstrating the septate cervix and high OVS with a small amount of hematocoele in the posterior space of the OVS (the arrow indicates the OVS). RUT, right uterus; LUT, left uterus; REN, right endometrium; LEN, left endometrium; RK, right kidney; LK, left kidney; RCX, right cervix; LCX, left cervix; UGTOIRA, unilateral genital tract obstruction with ipsilateral renal anomaly; OVS, oblique vaginal septum; TAS, transabdominal sonography; TRS, transrectal sonography; 2D, 2-dimensional; 3D, 3-dimensional.

of communication in the lower segment of the uterine cavity, the internal orifice of the cervix, and the cervical mediastinum was 100%, and the missed diagnosis rate was 0. The ultrasonic detection rate of the hole on the OVS was 0, and the missed diagnosis rate was 100%. The small hole in the OVS was easily found during the operation, but was difficult to detect with preoperative ultrasound. When cervical canal dilatation was accompanied by hemorrhage (effusion), the communicating fistula between two sides of the cervix septum could be easily detected using ultrasound; however, if the preoperative imaging examination did not indicate the intercervical communication, the surgeon overlooked the intercervical communication examination during vaginal oblique septectomy or cervicoplasty. When there was communication in the lower segment of the uterine cavity or the internal orifice of the cervix, the

ultrasound was characterized by the fusion of the intima on both sides in the lower segment of the uterine cavity or the internal orifice.

In this study, there were 13 cases (22.0%) of hematosalpinx, 1 case (1.7%) of pelvic hematocoele, 2 cases (3.4%) of hemoperitoneum, 2 cases (3.4%) of adenomyoma, 2 cases (3.4%) of adenomyoma with ipsilateral ovarian endometriosis cyst, and 6 cases (10.2%) of ipsilateral ovarian endometriosis cyst detected with SSUS and confirmed by surgery. This indicated that most patients with UGTOIRA syndrome were the communication type, and no-communication patients sought medical treatment, a timely diagnosis, and early treatment early and had a low probability of complications due to their early and severe symptoms. UGTOIRA syndrome of the communicating type, especially in those with cervical atresia and high OVS, is

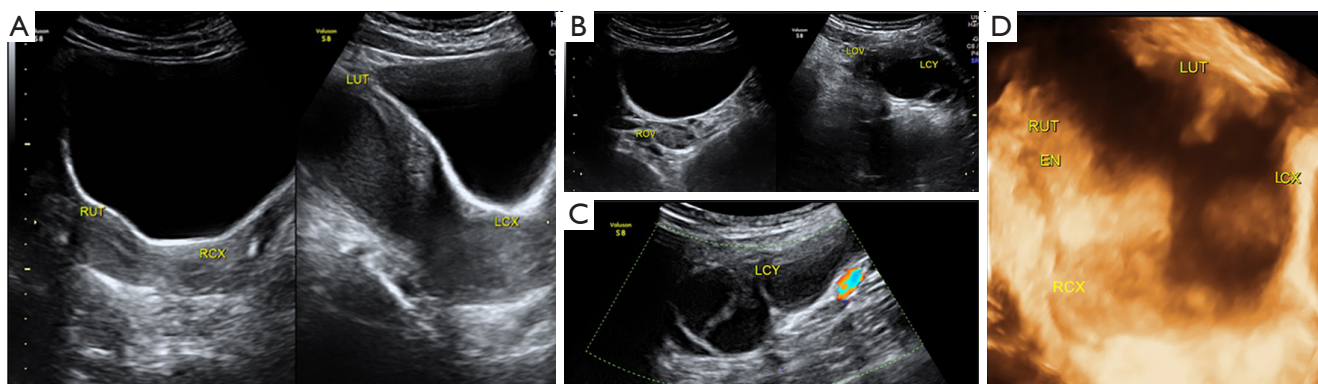


Figure 10 Type II-b UGTOIRA syndrome: U3b-C3b-V0, complete bicorporal uterus, double cervix with left obliterated external cervical orifice, with a normal vagina, without communication, hemorrhage filled in the left uterine cavity and cervical canal, left ovary with an endometriotic cyst, left hematosalpinx, and left renal agenesis. Sonograms were obtained from a 19-year-old female patient after the second operation, and the ultrasonic findings before the first 2 operations were the same as those from this ultrasonic examination (because the first operation was performed for the left-high OVS and the left external cervical orifice atresia, the adhesion atresia of the OVS and the external cervical orifice occurred after the operation, and the same situation occurred after the second operation). (A) TAS 2D sagittal pelvic planes demonstrating a normal right uterus, cervix, and vagina (left side of the figure), dense floating echogenic dots in the left uterine cavity and cervical canal with obliterated external cervical orifice (right side of the figure). (B) TAS 2D sagittal sections of the bilateral ovaries demonstrating a normal right ovary and a left ovary with an endometriotic cyst. (C) TAS 2D sagittal planes demonstrating left hematosalpinx. (D) TAS 3D coronal plane of the uterus under stereoscopy demonstrating complete bicorporal uterus, double cervix with left obliterated external cervical orifice, and hemorrhage filling in the left uterine cavity and cervical canal. RUT, right uterus; RCX, right cervix; LUT, left uterus; LCX, left cervix; ROV, right ovary; LOV, left ovary; LCY, left cyst; EN, endometrium; UGTOIRA, unilateral genital tract obstruction with ipsilateral renal anomaly; OVS, oblique vaginal septum; TAS, transabdominal sonography; 2D, 2-dimensional; 3D, 3-dimensional.

often not considered in clinic, owing to the lack of obvious symptoms of menstrual obstruction and other related complications. Ultrasonography as a first-line examination should improve the detection rate of UGTOIRA syndrome; if there is no early diagnosis and early treatment in the future, the clinical treatment of the poor pregnancy on the obstructive side will be difficult, and the cervical tumor on the obstructive side will be hard to detect for early diagnosis and early treatment.

In this study, all cases (100%) showed ipsilateral renal agenesis, which was reported in 95.4% of adolescents or adults (3). However, in a clinical study of UGTOIRA syndrome in prepubertal patients, ipsilateral renal anomaly showed as a multicystic dysplastic kidney (MCDK) (19). A study reviewing the MRI features of UGTOIRA syndrome reported that paravaginal cystic structure was found in 12.8% of patients (14). In our study, ultrasound detected 3 cases of paracervical cystic structure inserting into the cervix or vagina on the side of vaginal obstruction, which was possibly a mesonephric duct cyst or ureter remnant but was not confirmed by surgery. Because most paracervical

or paravaginal cystic structures are usually small, do not cause symptoms in patients with UGTOIRA syndrome, and do not need to be removed, there remains a lack of pathological evidence to confirm their nature.

SSUS can be used to accurately evaluate uterine malformations, cervical malformations, vaginal malformations, obstruction sites, the locations and volumes of keratocele, communications and communication sites, and ovarian endometriosis cysts in patients with UGTOIRA syndrome, as well as ipsilateral urinary system malformations. In order to improve the sensitivity and overall diagnosis of UGTOIRA syndrome and related complications, ultrasound doctors should understand and consider the etiology, embryological basis, and pathogenesis of UGTOIRA syndrome. We agree with the hypothesis that at about the sixth week of embryonic development, the development of the ipsilateral vagina stops when the caudal development of the unilateral mesonephric tube stops, resulting in the failure of the development of ureteral buds and kidneys on the ipsilateral side, which in turn leads to abnormal development of the uterus (20). Unilateral outlet

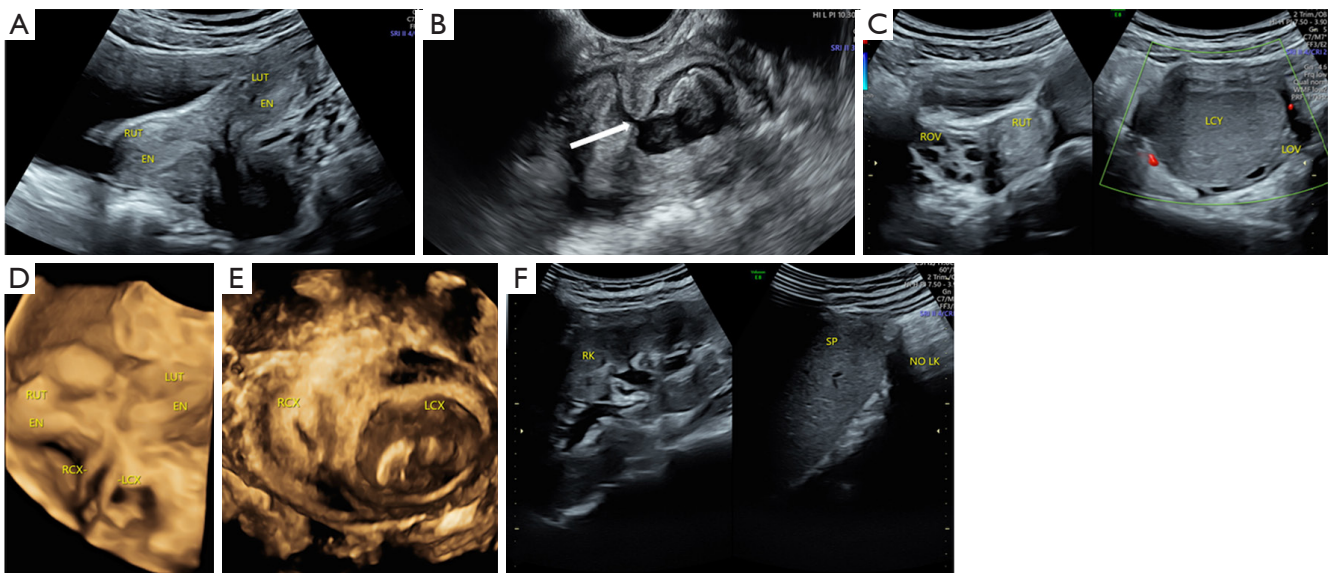


Figure 11 Type III UGTOIRA syndrome: U3c-C3b-V0, bicorporal septate uterus, septal cervix with left obliterated external cervical orifice, a fistula on the cervical septum, hemorrhage filling in the left cervical canal, a normal vagina, left ovary with an endometriotic cyst, and left renal agenesis. Sonograms were obtained from a 17-year-old female patient. (A) TAS 2D coronal plane demonstrating a bicorporal septate uterus and septal cervix. (B) TRS 2D cross-section of the cervix demonstrating the fistula on the cervical septum (the arrow indicates the fistula). (C) TAS 2D ovarian sagittal planes demonstrating a normal right ovary (left side of the figure) and an endometriosis cyst within the left ovary (right side of the figure). (D) TAS 3D coronal plane of the uterus-cervix under stereoscopy demonstrating a bicorporal septate uterus and septal cervix with left obliterated external cervical orifice and hemorrhage filling in the left cervical canal. (E) TRS 3D coronal plane of the cervix under stereoscopy demonstrating a septal cervix with left obliterated external cervical orifice and hemorrhage filling in the left cervical canal. (F) TAS 2D sagittal planes identifying the absence of the left kidney (NO LK; right side of the figure) and a normal right kidney (RK; left side of the figure). RUT, right uterus; LUT, left uterus; EN, endometrium; ROV, right ovary; LCY, left ovarian cyst; LOV, left ovary; RCX, right cervix; LCX, left cervix; RK, right kidney; SP, spleen; LK, left kidney; UGTOIRA, unilateral genital tract obstruction with ipsilateral renal anomaly; TAS, transabdominal sonography; TRS, transrectal sonography; 2D, 2-dimensional; 3D, 3-dimensional.

obstruction of the genital tract leads to menstrual reflux, and long-term persistent menstrual reflux is closely related to the occurrence and development of pelvic endometriosis and pelvic adhesion (8,21,22).

The advantage of this study is that it provides a detailed description of the SSUS ultrasonographic features of the genitourinary anatomical variations in UGTOIRA syndrome of a relatively large sample. The main limitations of this study are as follows: (I) the sample size was not sufficiently large, and some cases of UGTOIRA syndrome in our center were excluded because they did not allow SSUS examination; (II) patients without obvious symptoms of obstruction were not examined with laparoscopy or laparotomy and/or hysteroscopy, and in some cases, cervical communication, ureteral abnormalities, and paravaginal cystic structures could not be confirmed via operation or histopathology. In future research, more cases will be

needed to verify the application value of SSUS in the diagnosis of UGTOIRA syndrome and to determine more anatomic variations of UGTOIRA syndrome.

Conclusions

The results of this study indicated that ultrasound doctors with a certain theoretical knowledge of the embryology of the female genitourinary tract and rich experience in the ultrasonic diagnosis of female reproductive tract malformations can use standardized segmental sequential ultrasound procedures [joint application of transabdominal, transperineal, transvaginal, and transrectal ultrasound pathways (bidimensional and tridimensional)] to accurately evaluate uterine-cervical-vaginal malformations, obstruction sites, communication conditions, related complications, and renal hypoplasia of

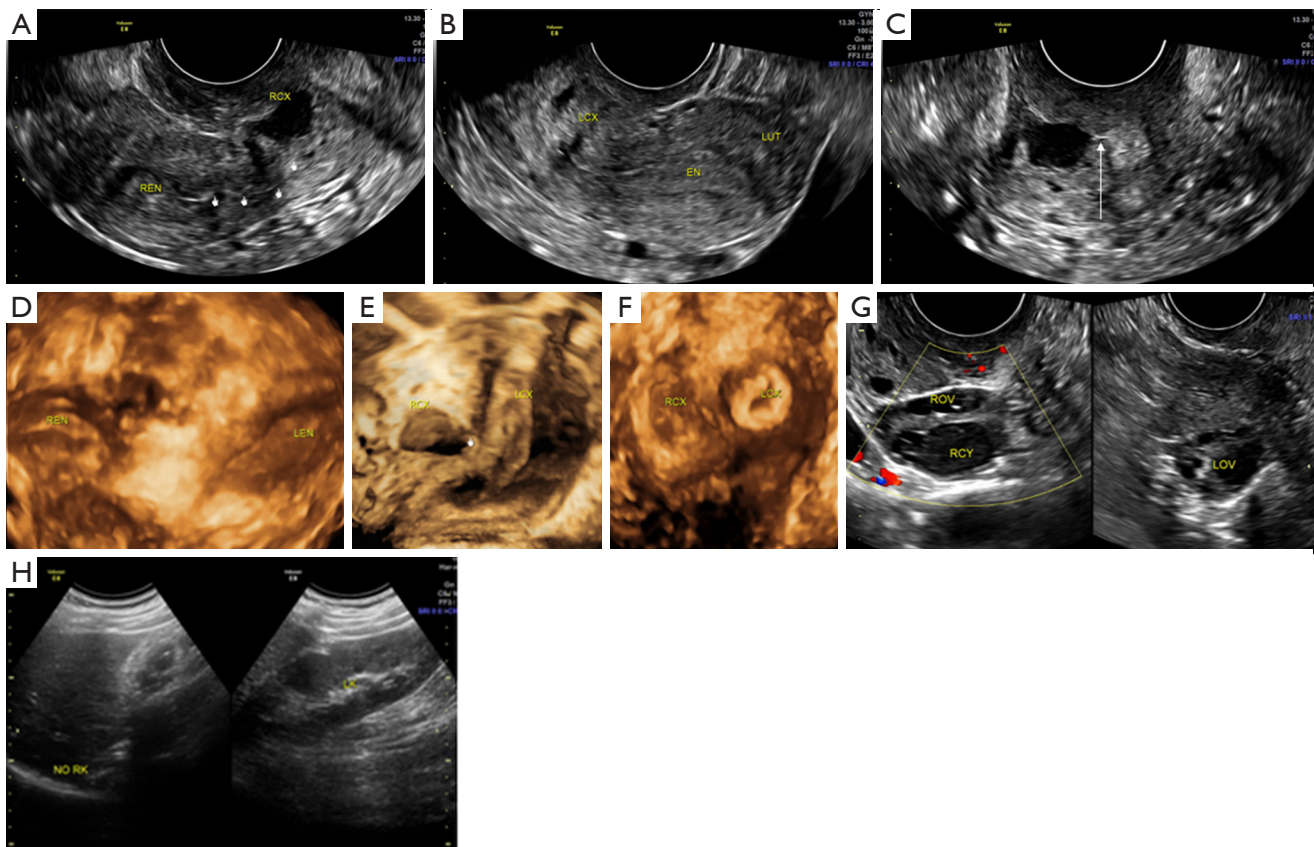


Figure 12 Type IV UGTOIRA syndrome: U3b-C3c-V0, complete bicorporal uterus, double cervix (partial cervical fusion) with right cervical canal effusion and obliterated external cervical orifice, with a normal vagina, with a fistula on the cervical fusion, endometrial cyst of the right ovary, and right renal agenesis. Sonograms were obtained from a 22-year-old female patient. (A) TVS 2D right uterine sagittal plane demonstrating a normal uterus, cervix with cervical canal effusion, and atresia of the external orifice (the hand arrows indicate that the cervical canal effusion continues with the uterine cavity). (B) TVS 2D left uterine sagittal plane demonstrating a normal uterus and cervix. (C) TVS 2D cross-section of the fused part of the double cervix (the arrow indicates the communication between the cervical canals on both sides). (D) TVS 3D coronal plane of the uterus under stereoscopy demonstrating a complete bicorporal uterus. (E) TVS 3D coronal plane of the cervix under stereoscopy demonstrating that the upper parts of the 2 cervixes are separated and that the lower parts of the 2 cervixes are fused, with the sinus visible in the fusion part (the hand arrow indicates the sinus). (F) TAS 3D cross-section of the fused part of the double cervix. (G) TAS 2D ovarian sagittal planes demonstrating an endometriosis cyst within the right ovary (left side of the figure) and a normal left ovary (right side of the figure). (H) TAS 2D sagittal planes identifying the absence of the right kidney (NO RK; left side of the figure) and a normal left kidney (LK; right side of the figure). REN, right endometrium; RCX, right cervix; LCX, left cervix; EN, endometrium; LUT, left uterus; LEN, left endometrium; ROV, right ovary; RCY, right ovarian cyst; LOV, left ovary; RK, right kidney; UGTOIRA, unilateral genital tract obstruction with ipsilateral renal anomaly; TVS, transvaginal sonography; 2D, 2-dimensional; 3D, 3-dimensional; TAS, transabdominal sonography.

UGTOIRA syndrome.

Acknowledgments

We would like to express our gratitude to all those who helped during the case collection and writing of this

manuscript, to the peer reviewers for their opinions and suggestions, and to the editors for their comments and guidance. We especially thank Mrs. Jing Cao, Rong Zhou, Yu Du, and Xizhi Wu (Department of Obstetrics and Gynecology of Tongji Hospital, Affiliated with Tongji Medical College of Huazhong University of Science and

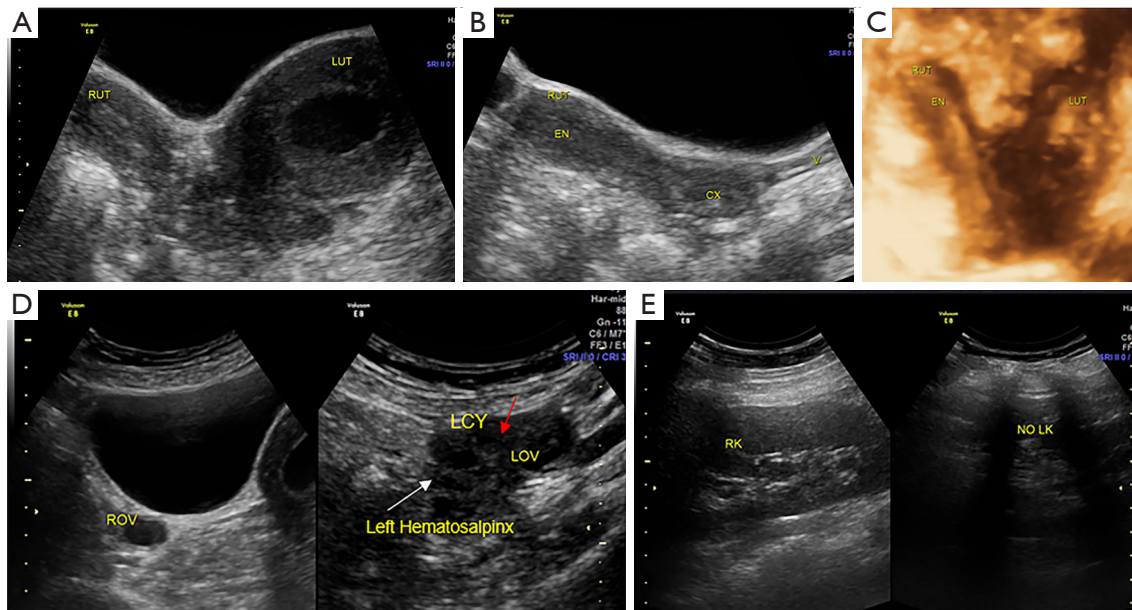


Figure 13 Type V UGTOIRA syndrome: U4a-C0-V0, left isthmus atresia with cavity hematometra and without communicating with right uterus, left completely undeveloped cervix, a normal vagina, left hematosalpinx, left ovarian endometriosis cyst, and left renal agenesis. Sonograms were obtained from a 15-year-old female patient. (A) TAS 2D coronal pelvic plane demonstrating the left isthmus atresia with cavity hematometra, no communication with the right uterus, and a completely undeveloped left cervix. (B) TAS 2D right uterine sagittal section demonstrating a normal uterus, cervix, and vagina. (C) TAS 3D coronal plane of the uterus under stereoscopy demonstrating the left isthmus atresia with cavity hematometra, no communication with the right uterus, and a completely undeveloped left cervix. (D) TAS 2D ovarian sagittal planes demonstrating normal right ovary (left side of the figure), a left ovarian endometrial cyst (a red arrow indicates a low echo), and a left hematosalpinx (a white arrow indicates a meandering low echo) beside the left ovary (right side of the figure). (E) TAS 2D sagittal planes identifying the absence of the left kidney (NO LK; right side of the figure) and a normal right kidney normal (RK; left side of the figure). RUT, right uterus; LUT, left uterus; EN, endometrium; CX, cervix; V, vagina; ROV, right ovary; LCY, left ovarian cyst; LOV, left ovary; RK, right kidney; LK, left kidney; UGTOIRA, unilateral genital tract obstruction with ipsilateral renal anomaly; TAS, transabdominal sonography; 2D, 2-dimensional; 3D, 3-dimensional.

Technology) for their help in the case collection.

Funding: This work was supported by the National Key R & D Program (the 14th Five-Year Plan) (No. 2022YFC2704000).

Footnote

Conflicts of Interest: All authors have completed the ICMJE uniform disclosure form (available at <https://qims.amegroups.com/article/view/10.21037/qims-23-204/coif>). The authors have no conflicts of interest to declare.

Ethical Statement: The authors are accountable for all aspects of the work in ensuring that questions related to the accuracy or integrity of any part of the work are appropriately investigated and resolved. This study was

conducted following the Declaration of Helsinki (as revised in 2013) and was a retrospective and descriptive analysis of the data collected prospectively for routine clinical services; individual consent for this retrospective analysis was thus waived. The study was approved by the Medical Ethics Committee of Tongji Hospital Affiliated to Tongji Medical College of Huazhong University of Science and Technology (No. TJ-IRB20220917).

Open Access Statement: This is an Open Access article distributed in accordance with the Creative Commons Attribution-NonCommercial-NoDerivs 4.0 International License (CC BY-NC-ND 4.0), which permits the non-commercial replication and distribution of the article with the strict proviso that no changes or edits are made and the original work is properly cited (including links to both the

formal publication through the relevant DOI and the license).
See: <https://creativecommons.org/licenses/by-nc-nd/4.0/>.

References

1. Wunderlich M. Unusual form of genital malformation with aplasia of the right kidney. *Zentralbl Gynakol* 1976;98:559-62.
2. Smith NA, Laufer MR. Obstructed hemivagina and ipsilateral renal anomaly (OHVIRA) syndrome: management and follow-up. *Fertil Steril* 2007;87:918-22.
3. Fedele L, Motta F, Frontino G, Restelli E, Bianchi S. Double uterus with obstructed hemivagina and ipsilateral renal agenesis: pelvic anatomic variants in 87 cases. *Hum Reprod* 2013;28:1580-3.
4. Ación P, Ación M. The presentation and management of complex female genital malformations. *Hum Reprod Update* 2016;22:48-69.
5. Bian ML. Oblique vaginal septum: report of 15 cases. *Zhonghua Fu Chan Ke Za Zhi* 1985;20:85-8, 126.
6. Purslow CE. A case of unilateral haematocolpos, haematometra, and haematosalpinx (letter). *J Obstet Gynecol Br Emp* 1922;29:643.
7. Cox D, Ching BH. Herlyn-Werner-Wunderlich syndrome: a rare presentation with pyocolpos. *J Radiol Case Rep* 2012;6:9-15.
8. Tong J, Zhu L, Chen N, Lang J. Endometriosis in association with Herlyn-Werner-Wunderlich syndrome. *Fertil Steril* 2014;102:790-4.
9. Aranke M, Nguyen KL, Wagner RD, Kauffman RP. Haematometrocolpos and acute pelvic pain associated with cyclic uterine bleeding: OHVIRA syndrome. *BMJ Case Rep* 2018;2018:bcr-2017-223348.
10. Schall K, Parks M, Nemivant S, Hernandez J, Weidler EM. Pelvic pain in patients with complex mullerian anomalies including Mayer-Rokitansky-Kuster-Hauser syndrome (MRKH), obstructed hemi-vagina ipsilateral renal anomaly (OHVIRA), and complex cloaca. *Semin Pediatr Surg* 2019;28:150842.
11. Shavell VI, Montgomery SE, Johnson SC, Diamond MP, Berman JM. Complete septate uterus, obstructed hemivagina, and ipsilateral renal anomaly: pregnancy course complicated by a rare urogenital anomaly. *Arch Gynecol Obstet* 2009;280:449-52.
12. Shah DK, Laufer MR. Obstructed hemivagina and ipsilateral renal anomaly (OHVIRA) syndrome with a single uterus. *Fertil Steril* 2011;96:e39-41.
13. Zhu L, Chen N, Tong JL, Wang W, Zhang L, Lang JH. New classification of Herlyn-Werner-Wunderlich syndrome. *Chin Med J (Engl)* 2015;128:222-5.
14. Zhang H, Ning G, Fu C, Bao L, Guo Y. Herlyn-Werner-Wunderlich syndrome: diverse presentations and diagnosis on MRI. *Clin Radiol* 2020;75:480.e17-25.
15. Zhang J, Xu S, Yang L, Songhong Y. MRI image features and differential diagnoses of Herlyn-Werner-Wunderlich syndrome. *Gynecol Endocrinol* 2020;36:484-8.
16. Gai YH, Fan HL, Yan Y, Cai SF, Zhang YZ, Song RX, Song SL. Ultrasonic evaluation of congenital vaginal oblique septum syndrome: A study of 21 cases. *Exp Ther Med* 2018;16:2066-70.
17. Liu M, Zhang L, Xia Y, Huang X, Ye T, Zhang Y, Qi Z, Wang L, Lai X, Dai Q, Jiang Y. New Consideration of Herlyn-Werner-Wunderlich Syndrome Diagnosed by Ultrasound. *J Ultrasound Med* 2021;40:1893-900.
18. Grimbizis GF, Gordts S, Di Spiezio Sardo A, Brucker S, De Angelis C, Gergolet M, Li TC, Tanos V, Brölmann H, Gianaroli L, Campo R. The ESHRE/ESGE consensus on the classification of female genital tract congenital anomalies. *Hum Reprod* 2013;28:2032-44.
19. Han JH, Lee YS, Im YJ, Kim SW, Lee MJ, Han SW. Clinical Implications of Obstructed Hemivagina and Ipsilateral Renal Anomaly (OHVIRA) Syndrome in the Prepubertal Age Group. *PLoS One* 2016;11:e0166776.
20. Aswani Y, Varma R, Choudhary P, Gupta RB. Wolffian Origin of Vagina Unfolds the Embryopathogenesis of OHVIRA (Obstructed Hemivagina and Ipsilateral Renal Anomaly) Syndrome and Places OHVIRA as a Female Counterpart of Zinner Syndrome in Males. *Pol J Radiol* 2016;81:549-56.
21. Abboud K, Giannini A, D'Oria O, Ramadan A, Ayed A, Laganà AS, Chiantera V, Sleiman Z. Laparoscopic Management of Rudimentary Uterine Horns in Patients with Unicornuate Uterus: A Systematic Review. *Gynecol Obstet Invest* 2023;88:1-10.
22. Bulletti C, Coccia ME, Battistoni S, Borini A. Endometriosis and infertility. *J Assist Reprod Genet* 2010;27:441-7.

Cite this article as: Zhang L, Liu R, Liu R, Wu M, Ye S. Diverse ultrasound image features of unilateral genital tract obstruction with ipsilateral renal anomaly syndrome on genitourinary system segmental sequential ultrasound screening and the accuracy of ultrasonic diagnosis. *Quant Imaging Med Surg* 2023;13(10):7194-7213. doi: 10.21037/qims-23-204